An analytical model for the Maxwell radiation field in an axially symmetric galaxy

Mayeul Arminjon

An analytical model for the Maxwell radiation field in an axially symmetric galaxy

Mayeul Arminjon

Univ. Grenoble Alpes, CNRS, Grenoble INP.

Laboratoire 3SR, Domaine universitaire,

BP53, 38041 Grenoble cedex 9, France.

Email: Mayeul.Arminjon@3sr-grenoble.fr

Abstract

An analytical model is built for the Maxwell field in an axisymmetric galaxy, especially that field which results from stellar radiation. This model is based on an explicit representation for axisymmetric free Maxwell fields. In a previous work, the general applicability of this representation has been proved. The model is adjusted by fitting to it the sum of spherical radiations emitted by the composing "stars". The huge ratio distance/wavelength needs to implement a numerical precision better than the quadruple precision. The model passes a validation test based on a spherically symmetric solution. The results for a set of "stars" representative of a disk galaxy indicate that the field is highest near to the disk axis, and there the axial component of **E** dominates over the radial one.

Keywords: Maxwell equations; axial symmetry; exact solutions; disk galaxy; numerical model.

1 Introduction

Apart from pure magnetic fields, which are thought to be produced by a galactic dynamo action [1, 2], the electromagnetic (EM) field in a galaxy is in the form of EM radiation. A lot of information can be found in the literature regarding the production of the EM radiation field by stars and by other astrophysical objects, its interaction with dust, as well as other processes of radiative transfer, or regarding the EM wave spectrum and its dependence on the position in the galaxy, etc. [3, 4]. However, it seems that little or nothing can be found about the description of the EM radiation field in a galaxy as an exact solution of the Maxwell equations. The aim of the present work is to propose and first check a method to obtain such relevant solutions.

Our main motivation for that work is to make a step towards testing the following prediction [8] of an alternative theory of gravity [9], which is a scalar theory with a preferred reference frame: In the presence of both a gravitational field and an EM field, the total energy(-momentum-stress) tensor is not the sum of the energy tensors of matter and the EM field – there must appear a specific interaction energy tensor, which should be distributed in space, and be gravitationally active. That energy could thus possibly contribute to the dark matter, because moreover it has an "exotic" character, being different from both the energy of matter and that of the EM field. (It has a classical nature, however, as has the theory [8, 9]. I.e., the theory does not say anything about the possibility that the interaction energy might result from underlying quantum particles.) The interaction energy tensor is characterized by a scalar (field), which is determined by the gravitational and EM fields in the preferred frame of the theory; hence it depends also on the velocity of the reference frame used, with respect to that preferred frame. More precisely, in order to calculate that scalar field in a weak and slowly varying gravitational field, one has to know the EM field and its first-order derivatives, as well as the time derivative $\partial_T U$ and the spatial gradient of the latter [8]. (Here U is the Newtonian potential.)

The precise goal of the present work, therefore, is to build a representative analytical model for the EM field in a galaxy – especially for the *spatio-temporal variation* of the EM field. This is in order to be able later to calculate the interaction energy predicted by the scalar theory [8], and to check if its distribution might have something common with a "dark halo". However, the present goal is to have the EM field in a galaxy as an exact solution of the Maxwell equations, and this is interesting *per se.* Section 2 describes the model that has been built in this work. Section 3 discusses its numerical implementation. The numerical results obtained so far are discussed in Sect. 4. Finally, we present our conclusions.

2 Description of the model

2.1 Main assumptions

The following lists and comments the essential assumptions of the model, i.e., the ones which it would be difficult to change without going to a different model:

(i) *The structure of the interstellar radiation field is determined by the sum of the EM radiation fields emitted by the stars.* This assumption actually defines the source input that we use to determine the parameters of a general solution of the Maxwell equations, see the end of this paragraph. It would be an oversimplifying assumption to equate this source input generally with the total interstellar radiation field, because this would mean neglecting the effect of important physical processes like dust extinction and, more generally, radiative transfer. Nevertheless, according to Maciel [4], "The interstellar radiation field in the optical and ultraviolet comes essentially from integrated stellar radiation". Note, moreover, that in directions which are roughly orthogonal to a galactic disk or at least are strongly inclined with respect to it, the light emitted by the stars of that galaxy will suffer much less alteration as compared with what happens close to the galactic plane. This is important in connection with the aim of checking if the "interaction energy" alluded to in the Introduction might significantly contribute to the dark matter halos, since, precisely, the most part of such a halo is outside the galactic disk. Even more important in this connection is an essential feature of our model: that it provides an EM field which is an exact solution of the Maxwell equations. In contrast, if one would try to account directly for absorption, emission, and scattering processes, this feature would be quite difficult to maintain. But on the other hand, in our model, the sum of the EM potentials generated by the point sources (by the "stars") is fitted by a general analytical solution, see the Theorem and see the statement of the model below. The sum just mentioned thus merely serves to determine the "shape" (the parameters) of that general solution. That analytical solution, in itself, is valid independently of whether the corresponding EM field has been generated directly or has undergone various radiative transfers.

(ii) *The distribution of the stars and (hence) the interstellar radiation field are axially symmetric.* This is of course not exactly true (cf. e.g. the arms of a spiral galaxy), but it seems to be a reasonable simplification which should provide a correct first approximation. Except for peculiar cases, e.g. if there we,re a correlation between the intensity of the EM radiation field emitted by a star and its angular position in the galaxy, and except for the vicinity of a star, the axisymmetry of the stars' distribution should indeed imply that of the interstellar radiation field. In any case, we shall assume that both the stars' distribution and the interstellar radiation field are axially symmetric.

(iii) *Each star emits a spherical radiation.* This assumption seems quite reasonable to describe the interstellar EM field at a large-enough distance from any individual star. Moreover, recall the discussion at the end of Point (i) above.

2.2 Distribution of the stars

- Each star (or bright object) is schematized as a point $\mathbf{x}$ determined by its cylindrical coordinates (ρ, ϕ, z): distance to the symmetry axis, azimuth, altitude, thus $\mathbf{x} = \mathbf{x}(\rho, \phi, z)$.

- A discrete set of such points, $\mathrm{S} = \{\mathbf{x}_i\} = \{\mathbf{x}(\rho_m, \phi_{mpq}, z_{mp})\}$ (that is, $i = i(m, p, q)$), is got by random generation, as follows:

  - An exponential distribution is assumed for $\rho > 0$, i.e., n_ρ values ρ_m $(m = 1, ..., n_\rho)$ are got by quasi-random generation with a probability:
  $$P(a < \rho_m < b) = \frac{1}{h} \int_a^b e^{-\frac{\rho}{h}} \mathrm{d}\rho, \tag{1}$$
  where h is the scale length, with $h = 3\,\mathrm{kpc}$ in the numerical computations, which roughly corresponds to the Milky Way [5, 6, 7].

  - Also, an exponential distribution is assumed for $z > 0$: for any $m = 1, ..., n_\rho$, we draw $n_z/2$ values z_{mp} (n_z being an even integer) by quasi-random generation with a probability law independent of m:

$$P(a < z_{mp} < b) = \frac{1}{h_z} \int_a^b e^{-\frac{z}{h_z}} \mathrm{d}z, \tag{2}$$

with $h_z = 0.2\,\mathrm{kpc}$ in the numerical computations.

- For each value $z_{mp} > 0$ thus obtained, we introduce another value $-z_{mp}$, i.e., we impose a perfect symmetry w.r.t. $z = 0$ in the distribution of z.
- Finally, for any two $m = 1, ..., n_\rho$ and $p = 1, ..., n_z$, we draw n_ϕ values ϕ_{mpq}, with a uniform distribution between 0 and 2π (thus ensuring the axial symmetry of the distribution of the "stars", as announced).

2.3 Explicit representation for axisymmetric EM fields

In Ref. [11], two classes of time-harmonic axisymmetric solutions of the free Maxwell equations were introduced, and it was shown that these two classes allow one to obtain in explicit form nonparaxial EM beams. The *first class of solutions* is got in the following way. One starts from a time-harmonic axisymmetric solution $\Psi(t, \rho, z) = e^{-\mathrm{i}\omega t}\hat{\Psi}(\rho, z)$ of the scalar wave equation, and one associates with it a vector potential $\mathbf{A}$ by

$$\mathbf{A} := \Psi \mathbf{e}_z, \qquad \text{or} \quad A_z := \Psi,\ A_\rho = A_\phi = 0. \tag{3}$$

(We shall denote by $(\mathbf{e}_\rho, \mathbf{e}_\phi, \mathbf{e}_z)$ the standard, point-dependent, direct orthonormal basis associated with the cylindrical coordinates ρ, ϕ, z.) In the time-harmonic case considered for the moment, such a vector potential defines uniquely [11, 12] the following exact solution of the Maxwell equations in free space:

$$B_\phi = -\frac{\partial A_z}{\partial \rho}, \qquad E_\phi = 0, \tag{4}$$

$$E_\rho = \mathrm{i}\frac{c^2}{\omega}\frac{\partial^2 A_z}{\partial \rho\, \partial z}, \qquad B_\rho = 0, \tag{5}$$

$$E_z = \mathrm{i}\frac{c^2}{\omega}\frac{\partial^2 A_z}{\partial z^2} + \mathrm{i}\omega A_z, \qquad B_z = 0. \tag{6}$$

In Ref. [11], this class was defined only when the scalar wave Ψ has the following form:

$$\Psi_{\omega\ S}\,(t,\rho,z) = e^{-\mathrm{i}\omega t} \int_{-K}^{+K} \ J_0\left(\rho\sqrt{K^2-k^2}\right)\ e^{\mathrm{i}k\,z}\, S(k)\,\mathrm{d}k, \tag{7}$$

with ω the angular frequency, $K := \omega/c$, [1] and J_0 the first-kind Bessel function of order 0. (c is the velocity of light.) This form does apply [10, 11] to any *totally propagating,* time-harmonic, axisymmetric solution of the scalar wave equation. However, as noted in Ref. [12], this form is not necessary at this stage and the solution (4)–(6) applies whether $A_z = \Psi$ is totally propagating or not.

The *second class of solutions* is deduced from the first one above by applying the EM duality to any solution of the first class, i.e., by setting [11]:

$$\mathbf{E}' = c\mathbf{B}, \quad \mathbf{B}' = -\mathbf{E}/c. \tag{8}$$

In the work [12], we showed that, by combining these two classes, one can define a method that allows one to get actually *all* totally propagating, time-harmonic, axisymmetric free Maxwell fields – and thus, by the appropriate summation on frequencies, all totally propagating axisymmetric free Maxwell fields. (The necessary restriction of the method to totally propagating fields turns out to be appropriate to describe the radiation field.) The main result that allows this is the following one:

Theorem [12]. *Let* $(\mathbf{A},\mathbf{E},\mathbf{B})$ *be any time-harmonic axisymmetric solution of the free Maxwell equations* (whether totally propagating or not). *There exist a unique solution* $(\mathbf{E}_1,\mathbf{B}_1)$ *of the first class (4)–(6) and a unique solution* $(\mathbf{E}'_2,\mathbf{B}'_2)$ *of the second class, both with the same frequency as has* $(\mathbf{A},\mathbf{E},\mathbf{B})$*, and whose sum gives just that solution:*

$$\mathbf{E} = \mathbf{E}_1 + \mathbf{E}'_2, \qquad \mathbf{B} = \mathbf{B}_1 + \mathbf{B}'_2. \tag{9}$$

Of course, as usual, it is implicit that, in Eqs. (4)–(6), B_ϕ, E_ρ and E_z are actually the *real parts* of the respective r.h.s. Therefore, when A_z is

[1] In Ref. [11], K was defined as $K := 2\omega/c$ instead.

totally propagating and hence has the form (7), we obtain (using the fact that $\mathrm{d}J_0/\mathrm{d}x = -J_1(x)$):

$$B_{\phi\,\omega\,S} = \mathcal{R}e\left[e^{-\mathrm{i}\omega t}\int_{-K}^{+K}\sqrt{K^2-k^2}\,J_1\left(\rho\sqrt{K^2-k^2}\right)\,S(k)\,e^{ikz}\mathrm{d}k\right], \tag{10}$$

$$E_{\rho\,\omega\,S} = \mathcal{R}e\left[-\mathrm{i}\frac{c^2}{\omega}e^{-\mathrm{i}\omega t}\int_{-K}^{+K}\sqrt{K^2-k^2}\,J_1\left(\rho\sqrt{K^2-k^2}\right)\mathrm{i}k\,S(k)\,e^{ikz}\mathrm{d}k\right], \tag{11}$$

$$E_{z\,\omega\,S} = \mathcal{R}e\left[\mathrm{i}e^{-\mathrm{i}\omega t}\int_{-K}^{+K}J_0\left(\rho\sqrt{K^2-k^2}\right)\left(\omega-\frac{c^2}{\omega}\,k^2\right)\,S(k)\,e^{ikz}\mathrm{d}k\right], \tag{12}$$

where $K := \omega/c$.

As we already mentioned, the case of a general time dependence is deduced from the case with harmonic time dependence by considering a frequency spectrum. We shall consider a discrete spectrum for simplicity. A totally propagating solution of the wave equation with a discrete frequency spectrum (ω_j) $(j = 1, ..., N_\omega)$ is got by summing solutions of the form (7):

$$\Psi_{(\omega_j)\ (S_j)}\,(t,\rho,z) = \sum_{j=1}^{N_\omega}\psi_{\omega_j\ S_j}\,(t,\rho,z), \tag{13}$$

where each $\psi_{\omega_j\ S_j}$ is a time-harmonic solution having the form (7). Note that the different frequencies do not necessarily have the same weight, since any given "wave vector spectrum" S_j can be multiplied by a factor w_j. In other words, the weights are contained in the functions S_j.

2.4 The case of spherical waves

The case of a *spherical* time-harmonic solution of the scalar wave equation is got by putting

$$S(k) \equiv \frac{c}{2\omega}\quad(-K < k < K\,) \tag{14}$$

in the axisymmetric time-harmonic solution (7): this yields [11, 13]

$$\psi_{\omega\ S\equiv\frac{c}{2\omega}}\,(t,\rho,z) = e^{-\mathrm{i}\omega t}\,\mathrm{sinc}\left(\frac{\omega}{c}r\right), \tag{15}$$

where $\operatorname{sinc}\theta := \frac{\sin\theta}{\theta}$, $\quad r := |\mathbf{x}| = \sqrt{\rho^2 + z^2}$.

If we have a set of spherical sources situated at the points $\mathbf{x}_i$, all sources having the same amplitude and the same frequency spectrum, (15) becomes:

$$\Psi_{(\mathbf{x}_i)\ (\omega_j)\ (S'_j)}\,(t, \rho, z) = \sum_{i=1}^{i_{\max}} \sum_{j=1}^{N_\omega} S'_j\, e^{-\mathrm{i}\omega_j t} \operatorname{sinc}\left(\frac{\omega_j}{c} r_i\right), \tag{16}$$

where $r_i := |\mathbf{x} - \mathbf{x}_i|$, and setting again the initial phases to zero for simplicity. Of course one might also make the amplitude of the source, as well as the weights affected to the different frequencies ω_j, depend on the source, i.e. on the index i, by giving a dependence on i to the positive numbers S'_j, which would thus become S'_{ij}.

2.5 The model

- Step **1**. Determine a relevant axisymmetric solution Ψ of the scalar wave equation, by fitting to the form (13) the sum (16) of the spherical radiations emitted by the "stars" that make the "galaxy".

- Step **2**.
    - (2.1) Calculate the associated EM field of the first class, (E_ρ, E_z, B_ϕ) with $B_\rho = B_z = E_\phi = 0$, by summing its time-harmonic contributions given by Eqs. (4)–(6), with $A_z := \Psi$, where Ψ is the result of step **1**.
    - (2.2) Similarly, calculate the associated EM field of the second class, (B'_ρ, B'_z, E'_ϕ) with $E'_\rho = E'_z = B'_\phi = 0$, by using the EM duality (8).

Step **1** (especially) is delicate numerically, as we will see in the next section. Therefore, we shall focus in this paper on Steps 1 and (2.1). Thus, *in the sequel of this paper, we shall omit step (2.2), i.e., we shall consider only solutions of the first class.* This means that we shall obtain axisymmetric EM fields having $B_\rho = B_z = E_\phi = 0$. "Complete" axisymmetric EM fields, obtained by summing solutions of the two classes, will of course have to be considered in the future work. At the stage of the fitting (Step 1), one may think to consider two different frequency spectra for the two classes, e.g. "mutually interpenetrating" ones.

3 Numerical implementation

3.1 Precise object of the fitting

The fitting of the sum (16) is done to determine the "wave vector spectra" S_j in Eq. (13):

$$\Psi_{(\omega_j)\ (S_j)}\,(t,\rho,z) = \sum_j \psi_{\omega_j\ S_j}\,(t,\rho,z), \tag{17}$$

where [Eq. (7) with $\omega = \omega_j$ and $K_j = \omega_j/c$]

$$\psi_{\omega_j\ S_j}\,(t,\rho,z) = e^{-\mathrm{i}\omega_j t} \int_{-K_j}^{+K_j} J_0\left(\rho\sqrt{\frac{\omega_j^2}{c^2} - k^2}\right)\, e^{\mathrm{i}k\,z}\, S_j(k)\,\mathrm{d}k. \tag{18}$$

Thus, we have one spectrum S_j for each value of the index $j = 1, ...N_\omega$, the latter specifying the frequency ω_j. To determine these spectra, several methods could be *a priori* envisaged. However, a difficulty comes from the huge ratio

$$\frac{\text{galactic distances}}{\text{wavelength}} \simeq \frac{\text{kpc}}{\mu\text{m}} \simeq 3\times 10^{25}, \tag{19}$$

which is the order of magnitude of the arguments of the Bessel function J_0 and the complex exponential in Eq. (18). This huge number discards several possibilities. First, it turns out to be not tractable at all here to determine each S_j by its Fourier coefficients C_{jn} – as proposed (for a very different problem) by Garay-Avendaño & Zamboni-Rached [11]. Indeed, considering (to begin with) one axisymmetric time-harmonic solution (7) of the scalar wave equation, this method leads to the following expansion {Eq. (8) in Ref. [11]}:

$$\psi_{\omega\ S}\,(t,\rho,z) = 2Ke^{-\mathrm{i}\omega t} \sum_{n=-\infty}^{\infty} C_n\,\mathrm{sinc}(h_{\omega\,n}(\rho,z)), \tag{20}$$

with $K = \omega/c$ and

$$h_{\omega\,n}(\rho,z) = \sqrt{K^2\rho^2 + (zK+\pi n)^2}. \tag{21}$$

Introducing the wavelength $\lambda = 2\pi c/\omega = 2\pi/K$, we have from (21):

$$(h_{\omega\,n}(\rho,z)))^2 = \pi^2\left[\left(\frac{2\rho}{\lambda}\right)^2 + \left(\frac{2z}{\lambda}+n\right)^2\right]. \tag{22}$$

On the r.h.s. of Eq. (22), ρ/λ and z/λ have the huge magnitude (19). Therefore, the functions $h_{\omega\, n}$, hence also the functions $\mathrm{sinc}(h_{\omega\, n})$ which form the basis in the expansion (20), are practically independent of n for relevant values of the spatial variables ρ and z, unless n would take similarly huge values. In that case, presumably, an integer of an akin value should give the number of the different values n to be taken in order to have an accurate expansion (20) – which of course is not tractable. Anyway, this method has been tried in this work and has not allowed us to get an accurate fitting of the sum (16).

A second method which is *a priori* conceivable to determine the "spectra" S_j in Eq. (13) by fitting the sum (16) to this equation, and has indeed been tried in this work, is by inverse Fourier transform: again, considering one axisymmetric time-harmonic solution (7) of the scalar wave equation, and removing its dependence in t, a formal inverse Fourier transform gives us

$$S(k) = \frac{1}{2\pi J_0\left(\rho\sqrt{K^2-k^2}\right)} \int_{-\infty}^{+\infty} \psi(\rho,z) e^{-ikz} \mathrm{d}z. \tag{23}$$

This should thus be independent of ρ when $e^{-\mathrm{i}\omega t}\psi(\rho,z)$ is indeed an axisymmetric time-harmonic solution, with frequency ω, of the wave equation. What we found numerically using the Matlab software is that, for the solution (15) corresponding to a spherical wave, with the frequency ω_0 being defined in Sect. 4 below: i) The spectrum S obtained by Eq. (23) depends on ρ, which it shouldn't. ii) For a given value of ρ, $S(k)$ varies with $k \in]-K,+K[$ instead of being the constant $S(k) \equiv \frac{c}{2\omega} = \frac{1}{2K}$. iii) For values of ρ in the investigated range $(10^{-3}\,\mathrm{kpc}, ..., 10^{2}\,\mathrm{kpc})$, $S(k)$ is much smaller than that value $\frac{1}{2K}$ – by a factor of at least 10^5 to 10^{10} at given ρ, and depending on ρ. We tried also to determine $S(k)$ using an inverse Fourier transform starting from the EM field instead of the EM potential A_z: e.g., starting from the component E_z [Eq. (12) in the time-harmonic case]. This also was not successful in the numerical application with the relevant numbers.

Instead, the method we finally used to determine S_j is by the values

$$S_{nj} := S_j(k_{nj}) \quad (n = 0, ..., N, \quad j = 1, ..., N_\omega), \tag{24}$$

where

$$k_{nj} = -K_j + n\delta_j \quad (n = 0, ..., N) \tag{25}$$

is a regular discretization of the integration interval $[-K_j, +K_j]$ for k, corresponding with the frequency ω_j, Eq. (18). (We remind that $K_j := \omega_j/c$; moreover, $\delta_j := 2K_j/N$ is the size of the discretization interval.) Using the so-called "Simpson $\frac{3}{8}$ composite rule", integrals like the one in Eq. (18) are approximated by discrete sums, as follows:

$$\int_{-K_j}^{+K_j} f(k)\mathrm{d}k = \sum_{n=0}^{N} a_{nj} f(k_{nj}) + O\left(\frac{1}{N^4}\right), \tag{26}$$

where N must be a multiple of 3, and

$$a_{nj} = (3/8)\,\delta_j \quad (n = 0 \text{ or } n = N), \tag{27}$$

$$a_{nj} = 2 \times (3/8)\,\delta_j \quad (\mathrm{mod}(n,3) = 0 \text{ and } n \neq 0 \text{ and } n \neq N), \tag{28}$$

$$a_{nj} = 3 \times (3/8)\,\delta_j \quad \text{otherwise.} \tag{29}$$

Using the approximation (26) to calculate Ψ [Eqs. (17) and (18)], we get:

$$\Psi(t,\rho,z) = \sum_{n=1}^{N} \sum_{j=1}^{N_\omega} f_{nj}(t,\rho,z)\, S_{nj} + O\left(\frac{1}{N^4}\right), \tag{30}$$

with

$$f_{nj}(t,\rho,z) = \frac{\omega_j}{\omega_0} a_n\, J_0\left(\rho \frac{\omega_j}{\omega_0}\sqrt{K_0^2 - k_n^2}\right) \exp\left[\mathrm{i}\left(\frac{\omega_j}{\omega_0} k_n z - \omega_j\, t\right)\right], \tag{31}$$

where the real numbers $a_n \geq 0$ and k_n $(0 \leq n \leq N)$ are as a_{nj} and k_{nj} in Eqs. (27) and (25, replacing K_j by $K_0 = \frac{\omega_0}{c}$, so that

$$a_{nj} = \frac{\omega_j}{\omega_0} a_n, \quad k_{nj} = \frac{\omega_j}{\omega_0} k_n. \tag{32}$$

To determine the spectra S_j, i.e. the unknown complex numbers (24), we fit the sum of the scalar potentials of the individual "stars", Eq. (16), by Eq. (30). To do that, we evaluate the sum (16) at a discrete set G of values of t, ρ and z, that makes a regular three-dimensional grid of points of spacetime:

$$G = \{(t_l, \rho_m, z_p),\ 1 \leq l \leq N_t,\ 1 \leq m \leq N_\rho,\ 1 \leq p \leq N_z\}. \tag{33}$$

We group the indices l, m, p as a single index $J = J(l,m,p)$ $(1 \leq J \leq J_{\max} = N_t \times N_\rho \times N_z)$. We denote the corresponding values of the sum (16) by D_J:

$$D_J = \sum_{i=1}^{i_{\max}} \sum_{j=1}^{N_\omega} S'_j\, e^{-\mathrm{i}\omega_j t_l}\, \mathrm{sinc}\left(\frac{\omega_j}{c}\left|\mathbf{x}(\rho_m, \phi = 0, z_p) - \mathbf{x}_i\right|\right). \tag{34}$$

(Recall that $\mathbf{x}(\rho, \phi, z)$ is the spatial point with cylindrical coordinates (ρ, ϕ, z).) Similarly, we denote $A_{J\ nj} = f_{nj}(t_l, \rho_m, z_p)$. The fitting of the sum (16) by Eq. (30) on the spatiotemporal grid G amounts to solving the linear system

$$\sum_{n=1}^{N} \sum_{j=1}^{N_\omega} A_{J\ nj}\, S_{nj} = D_J \quad (J = 1, ...J_{\max}) \tag{35}$$

in the sense of the least squares, hence getting the complex numbers S_{nj} as the output. These calculations are implemented on a PC, using the Matlab language and software.

3.2 Quadruple precision is needed

The ratio in Eq. (19), thus a number of the order of 10^{25}, gives the magnitude of the argument of the sinc function in Eq. (16) and the argument of the Bessel function J_0 in Eq. (18). However, the sinc and Bessel J_0 functions oscillate around 0 with a pseudo-period which is of the order of unity (exactly 2π, for sinc). So already to get only the correct *sign,* one needs to know their arguments to a precision better than $O(1)$. In view of the magnitude of the arguments: $O(10^{25})$, it means that 25 significant digits are needed to know just the sign of $\mathrm{sinc}\left(\frac{\omega_j}{c} r_i\right)$ in Eq. (16) and the sign of $J_0\left(\rho\sqrt{\frac{\omega_j^2}{c^2} - k^2}\right)$ in Eq. (18). Therefore, double precision (16 significant digits) is not enough: quadruple precision (32 significant digits) is needed – and even, it is not a luxury. Implementing quadruple precision, using the Matlab function `vpa` (for "variable precision arithmetic"), increases drastically the computation time. But, fortunately, we could reduce significantly the computation time (by a factor of approximately 20 for our programs), by using the external toolbox "Multiprecision Computing Toolbox for Matlab", of Advanpix. In that toolbox, we imposed the number of digits to be 41, in order to reach the same level of numerical precision as with the Matlab function `vpa` with default precision, i.e., 32 digits plus 9 "guard digits". [2]

3.3 Calculation of the EM field and its exact character

As with Eq. (17) and (18) for the A_z potential: each of B_ϕ, E_ρ, and E_z is the sum of the time-harmonic components given by Eqs. (10)–(12). And as

[2] This was advised to the author by Pavel Holoborodko, of Advanpix.

we did with A_z to obtain Eqs. (30) and (31), we use the approximation (26) to calculate the integrals in Eqs. (10)–(12). We thus get:

$$B_\phi(t,\rho,z) = \sum_{n=1}^{N}\sum_{j=1}^{N_\omega} R_n\, J_1\left(\rho\frac{\omega_j}{\omega_0}R_n\right)\, \mathcal{R}e\left[F_{nj}(t,z)\right] + O\left(\frac{1}{N^4}\right), \tag{36}$$

$$E_\rho(t,\rho,z) = \sum_{n=1}^{N}\sum_{j=1}^{N_\omega} \frac{c^2}{\omega_0}k_n R_n\, J_1\left(\rho\frac{\omega_j}{\omega_0}R_n\right)\, \mathcal{R}e\left[F_{nj}(t,z)\right] + O\left(\frac{1}{N^4}\right), \tag{37}$$

$$E_z(t,\rho,z) = \sum_{n=1}^{N}\sum_{j=1}^{N_\omega} \left(\frac{c^2}{\omega_0}k_n^2 - \omega_0\right)\, J_0\left(\rho\frac{\omega_j}{\omega_0}R_n\right)\, \mathcal{I}m\left[F_{nj}(t,z)\right] + O\left(\frac{1}{N^4}\right), \tag{38}$$

with $R_n = \sqrt{K_0^2 - k_n^2}$ and

$$F_{nj}(t,z) = \left(\frac{\omega_j}{\omega_0}\right)^2 a_n \exp\left[\mathrm{i}\left(\frac{\omega_j}{\omega_0}k_n z - \omega_j\, t\right)\right] S_{nj}. \tag{39}$$

Suppose one starts from an exact solution, with a discrete frequency spectrum (ω_j), of the scalar wave equation: $A_z = \Psi_{(\omega_j)\ (S_j)}$ given by Eqs. (17) and (18) with exact "wave-vector spectra" S_j. Then Eqs. (36)–(38) for the EM field give in general only an approximation of the associated EM field (defined by summing the contributions (10)–(12)): this is due to the discrete integration method (26), using the discrete values (24) of the exact functions S_j.

However, the integration formula (26) is *exact* (i.e., the remainder is not only $O(1/N^4)$ but exactly zero) if the integrand function f is a polynomial of degree ≤ 3. This is because the remainder is proportional to $f^{(4)}(\xi)$ for some $\xi \in]-K_j, +K_j[$ [14]. Moreover, given e.g. the first four arguments k_{nj} and the four corresponding function values S_{nj} ($n = 0, ..., 3$), there exists one and only one polynomial P of degree ≤ 3, such that $P(k_{nj}) = S_{nj}$ ($n = 0, ..., 3$). (This is the well-known "Unisolvence theorem"; note that we are considering a fixed value of the frequency index j.) By construction, N is a multiple of 3, hence the whole integration interval $[-K_j, +K_j]$ is the union of $N/3$ adjacent subintervals, each covering three steps δ_j. Thus, due to the unisolvence theorem: in each of those subintervals, the four successive arguments k_{nj} and the four corresponding function values S_{nj} define a unique 3rd-degree polynomial, for which the integration (26) is exact. It follows that the integration (26) is exact for the piecewise polynomial function $\widetilde{S}_j$ which continuously extends those $N/3$ polynomial functions to the whole interval $[-K_j, +K_j]$. [3] Therefore, Eqs. (30) and (31) actually define an exact solution $\widetilde{\Psi}$ of the scalar wave equation, which corresponds with substituting the functions $\widetilde{S}_j$ for S_j in Eqs. (17) and (18). Similarly, Eqs. (36)–(38) for the EM field give the exact result of adding the contributions (10)–(12) for the different frequencies ω_j, when in these contributions one considers, for the frequency $\omega = \omega_j$, the spectrum function $S = \widetilde{S}_j$. In other words, *Eqs. (36)–(38) provide an exact solution of the free Maxwell equations, deduced from an exact solution (30) of the scalar wave equation* – all corresponding with the spectrum functions $\widetilde{S}_j$, which are piecewise 3rd-degree polynomials.

3.4 Validation test

The formulas (30) and (36)–(38) were implemented numerically and that numerical implementation was tested for the case with spherical symmetry, as follows. We can define an exact solution of the free Maxwell equations by Eqs. (4)–(6), with $A_z = \psi_{\omega\ S\equiv\frac{c}{2\omega}}$ the spherically-symmetric time-harmonic solution (15) of the scalar wave equation. This yields (after taking the real part):

$$B_\phi(t,\rho,z) = \rho\cos\omega t\,\left(\frac{\sin Kr}{r^3} - K\frac{\cos Kr}{r^2}\right), \tag{40}$$

$$E_\rho(t,\rho,z) = \frac{c^2}{\omega}\frac{\rho z}{r^3}\sin\omega t\left[-\frac{3K}{r}\cos Kr + \left(\frac{3}{r^2} - K^2\right)\sin Kr\right], \tag{41}$$

[3] The continuity of $\widetilde{S}_j$ results from the common value S_{nj} at the common bound of any two successive subintervals. (The derivatives of $\widetilde{S}_j$ are in general not continuous at the bounds of the subintervals, though.) Note that the integration formula (26) gives the same result whether it is applied to the whole interval, or successively to each of the subintervals, each covering three steps δ_j, because the weights $a_{nj} = (3/8)\,\delta_j$ at the bounds of two successive subintervals add to give the weight $a_{nj} = 2\times(3/8)\,\delta_j$ at a multiple of three steps inside the whole interval.

$$E_z(t,\rho,z) = \frac{c^2}{\omega}\frac{\sin\omega t}{r}\left[\frac{K}{r}\left(1-\frac{3z^2}{r^2}\right)\cos Kr + \left(\frac{3z^2}{r^4} - \frac{1+K^2z^2}{r^2} + K^2\right)\sin Kr\right], \tag{42}$$

with $K := \omega/c$ and $r := \sqrt{\rho^2+z^2}$. The outputs of the (exact) Eqs. (40)–(42) were compared to those of Eqs. (36)–(38) applied with the relevant constant spectrum $S(k) := \frac{c}{2\omega}$, thus in Eq. (39):

$$S_n := S(k_n) = \frac{c}{2\omega} \quad (n = 0, ..., N). \tag{43}$$

(We are considering the single angular frequency case: $N_\omega = 1$, hence the index j is omitted since it takes only one value: $j = 1$; moreover, we set $\omega_1 := \omega_0 := \omega$ in Eqs. (36)–(39).) Note that, with the exact spectrum $S(k) := \frac{c}{2\omega}$, Eqs. (10)–(12) provide *just the same* exact fields as do Eqs. (40)–(42). However, even with the exact spectrum values (43), Eqs. (36)–(38) provide only an approximation of *those* exact fields, due to the discrete integration (26).

Figs. 1 to 3 show, for the three different scales investigated, the relative average quadratic differences between the fields $\Psi = A_z$, B_ϕ, E_ρ, E_z, as calculated either "directly", i.e., by Eqs. (15) and (40)–(42), or "with the spectrum (43)", i.e., by Eqs. (30) and (36)–(38) applied with the spectrum values (43). The different scales were here: $\texttt{scale} = 10^n\lambda$ $(n = 1, 2, 3)$, with $\lambda := c/\nu$. For this test, the frequency was taken to be $\nu := \omega/(2\pi) = 100\,\text{MHz}$, thus $\lambda = 3\,\text{m}$. The average quadratic differences are in general evaluated on a regular three-dimensional spatio-temporal grid (33) for the variables t, ρ, z. Thus t takes N_t values between t_0 and $t_0 + (N_t - 1)\delta t$, ρ takes N_ρ values between ρ_0 and $\rho_0 + (N_\rho - 1)\delta\rho$, and z takes N_z values between z_0 and $z_0 + (N_z - 1)\delta z$, with $\delta t = T/N_t$, $\delta\rho = \texttt{scale}/N_\rho$, and $\delta z = \texttt{scale}/(10N_z)$. However, in the present case with harmonic time dependence, we took $N_t = 1$, thus one value of $t = t_0$, which was fixed at $T/8$, with $T = 1/\nu = 10^{-8}\,\text{s}$. So here the grid is two-dimensional in fact. Also, we took here $N_\rho = 14$, $N_z = 13$, and $\rho_0 = \delta\rho$, $z_0 = 5\delta z$.

As expected, the errors (the relative delta's on the different fields calculated either "directly" or "with the spectrum (43)") decrease strongly as the discretization of the (here constant) spectrum function $S(k)$ becomes finer,

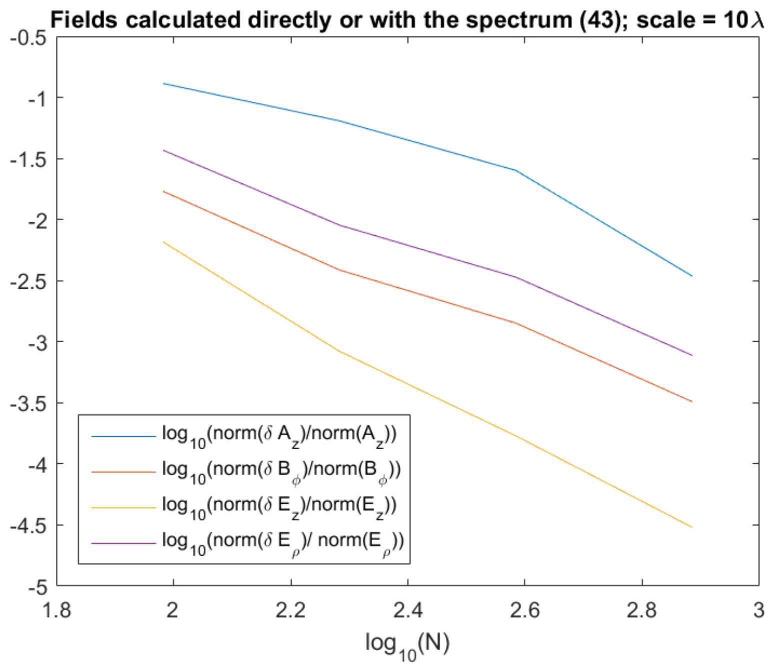

Figure 1: Average quadratic differences on a (ρ, z) grid. Scale: 10λ

i.e., with increasing N. (See Eq. (24).) *This validates the correctness of our calculations.* However, the errors increase quickly when the scale length `scale` is increased (even though it remains here enormously smaller than the galactic scale). This is because the integrals in Eqs. (18) and (10)–(12) involve functions of k that oscillate with a frequency or a pseudo-frequency which is proportional to the magnitude of the spatial variables ρ and z. As these integrals are approximated by the discrete sums (30) and (36)–(38), one would have to increase the discretization number N in proportion of the scale length `scale`.

This test of Eqs. (36)–(38) by an exact solution with spherical symmetry can be extended to the case of a set of spherical sources situated at the points $\mathbf{x}_i$. That is, one defines an exact solution of the free Maxwell equations by Eqs. (4)–(6), with $A_z = \Psi_{(\mathbf{x}_i)\ (\omega_j)\ (S'_j)}$ as given by Eq. (16). (Thus, all sources have the same amplitude and the same frequency spectrum, but this can easily be changed.) The fields produced by the source at $\mathbf{x}_i$ are denoted by $B_{\phi\, i}$, $E_{\rho\, i}$ and $E_{z\, i}$, and are given by Eqs. (40)–(42) [see Eq. (49), though],

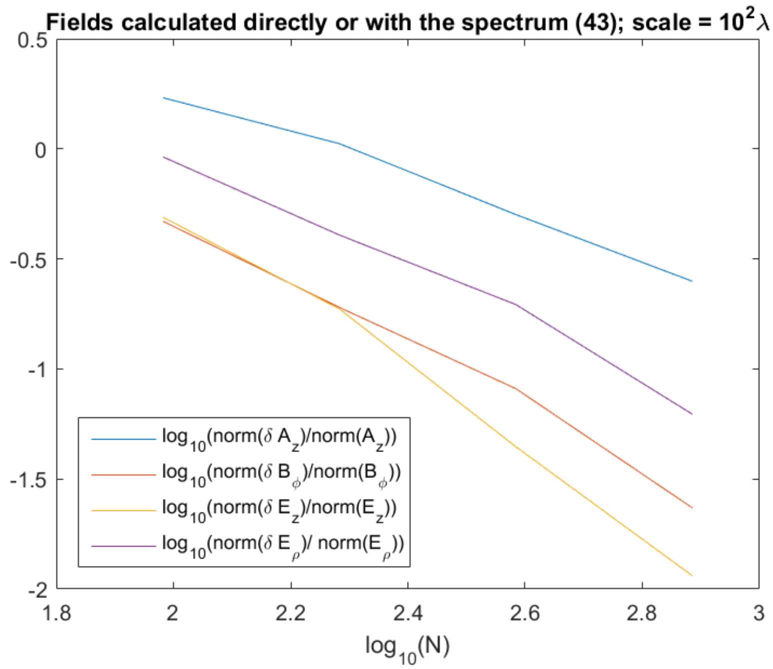

Figure 2: Average quadratic differences on a (ρ, z) grid. Scale: $10^2\lambda$

but with ρ, z and r being replaced by

$$\rho'_i := \sqrt{(x-x_i)^2 + (y-y_i)^2}, \tag{44}$$

$$Z_i := z - z_i, \tag{45}$$

$$r_i := |\mathbf{x} - \mathbf{x}_i| = \sqrt{(x-x_i)^2 + (y-y_i)^2 + (z-z_i)^2} = \sqrt{\rho'^2_i + Z_i^2}. \tag{46}$$

Thus, the definition of $B_{\phi\, i}$, $E_{\rho\, i}$ and $E_{z\, i}$ is that the exact fields produced at $\mathbf{x}$ by the source at $\mathbf{x}_i$ are decomposed on the orthonormal direct basis made of

$$\mathbf{e}'_{\rho\, i} = \mathbf{e}'_\rho(\mathbf{x}; \mathbf{x}_i) = \left((x-x_i)\mathbf{e}_x + (y-y_i)\mathbf{e}_y\right)/\rho'_i, \tag{47}$$

$$\mathbf{e}'_{\phi\, i} = \mathbf{e}'_\phi(\mathbf{x}; \mathbf{x}_i) := \mathbf{e}_z \wedge \mathbf{e}'_\rho(\mathbf{x}; \mathbf{x}_i) = \left((x-x_i)\mathbf{e}_y - (y-y_i)\mathbf{e}_x\right)/\rho'_i, \tag{48}$$

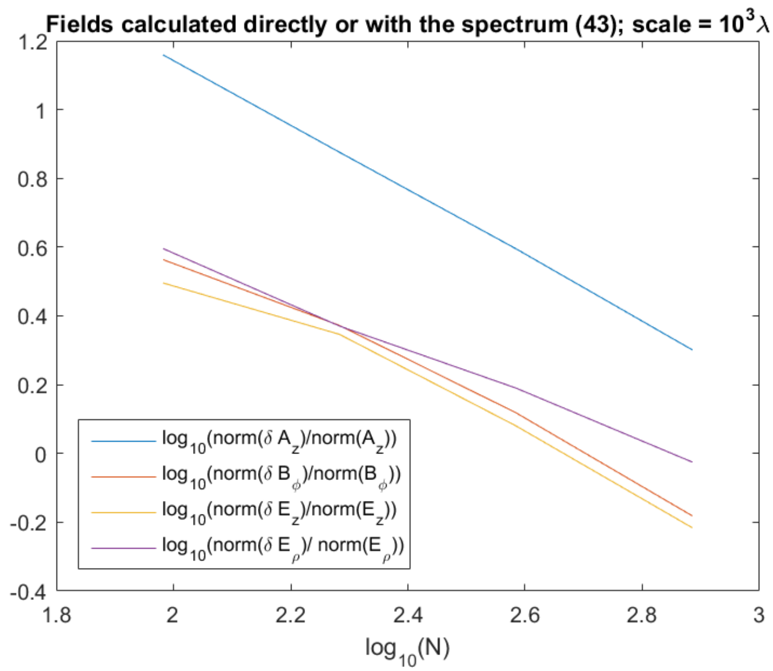

Figure 3: Average quadratic differences on a (ρ, z) grid. Scale: $10^3\lambda$

and $\mathbf{e}_z$. When each spherical source has the same discrete frequency spectrum (ω_j, S'_j), as in Eq. (16), it is understood that the components $B_{\phi\, i}$, $E_{\rho\, i}$ and $E_{z\, i}$ involve the corresponding weighted sum, e.g.

$$B_{\phi\, i} = \sum_{j=1}^{N_\omega} S'_j \; B_{\phi\, i\, \omega_j}, \tag{49}$$

where $B_{\phi\, i\, \omega_j}$ is given by Eq. (40) with $\rho'_i, Z_i, r_i, \omega_j, K_j$ in the place of ρ, z, r, ω, K. The total exact fields, sums of these different fields, are (reminding that $B_{\rho\, i} = B_{z\, i} = E_{\phi\, i} = 0$):

$$B_\phi := \mathbf{B}.\mathbf{e}_\phi = \sum_i B_{\phi\, i}\, \mathbf{e}'_{\phi\, i}.\mathbf{e}_\phi, \tag{50}$$

$$E_\rho := \mathbf{E}.\mathbf{e}_\rho = \sum_i E_{\rho\, i}\, \mathbf{e}'_{\rho\, i}.\mathbf{e}_\rho, \tag{51}$$

$$E_z := \mathbf{E}.\mathbf{e}_z = \sum_i E_{z\, i}. \tag{52}$$

In general, the other components of the total fields may be non-zero also, but we assume that the distribution of the identical spherical sources is axisymmetric (see Sect 2.2). In that case, the potential $A_z = \Psi$ in Eq. (16) is axisymmetric, too, hence, by Eqs. (4)–(6), we have $E_\phi = B_\rho = B_z = 0$. Note also that $\mathbf{e}_\rho$ and $\mathbf{e}_\phi$, hence also the scalar products in Eqs. (50)–(51), and therefore also the B_ϕ and E_ρ components, are not defined if $\rho = 0$.

4 Results and discussion

A file of some 10^4 randomly generated "stars" (as described in Subsect. 2.2) has been used here, more precisely one with $16 \times 16 \times 36$ triplets (ρ, z, ϕ).

The angular frequencies ω_j are the same in the expression to be fitted, Eq. (16), and in the analytical expression used to fit it, Eq. (17). They are regularly spaced and symmetric around a central frequency ω_0, thus

$$\omega_j = \omega_0 - \Delta\omega + (j-1)\frac{\Delta\omega}{N_{\mathrm{inter}}}, \quad (j = 1, ..., N_\omega = 2N_{\mathrm{inter}} + 1), \tag{53}$$

where $\omega_0 = \frac{2\pi c}{\lambda_0}$, $\Delta\omega < \omega_0$. In the calculations, we took $N_{\mathrm{inter}} = 5$ (hence $N_\omega = 11$), $\lambda_0 := 0.5\,\mu\mathrm{m}$, $\Delta\omega = \omega_0/2$. The weights S'_j affected to the different frequencies in Eq. (16) have the form

$$S'_j \propto \omega_j \exp\left[-\frac{1}{2\sigma^2}\left(\omega_j - \omega_0\right)^2\right] \quad (j = 1, ..., N_\omega) \tag{54}$$

with $\sigma = \Delta\omega$, and are normed so that $\sum_j S'_j = 1$.

A few different spacetime domains (variables t, ρ, z) of galactic dimensions have been used. The adopted sizes of the domain for the calculations discussed here were as follows:

$$0 \;\leq\; t \;<\; T_0 \;:=\; \frac{\lambda_0}{c}, \tag{55}$$

$$\rho_0 \;\leq\; \rho \;< \texttt{scale}\;, \tag{56}$$

$$-\texttt{scale}/20 \;<\; z \;< \texttt{scale}/20, \tag{57}$$

with $\texttt{scale} = 3.086 \times 10^{20}\,\mathrm{m} \;\simeq\; 10\,\mathrm{kpc}$ and $\rho_0 = \texttt{scale}/10^6$ in these calculations.

We have discretized that domain using grids (33) with $N_t = 4, \quad N_\rho = 8, \quad N_z = 7$ – in short $(4, 8, 7)$ —, or $(5, 12, 11)$, or $(7, 14, 13)$. The symbols $\leq$ and $<$ in Eqs. (55)–(57) are meant to indicate that, e.g. for Eq. (55), the discrete variation of t begins with $t = 0$ and ends with the largest multiple of the time step that is smaller than T_0. The time step is $\delta t = T_0/N_t$, so $t = (i_t - 1)\delta t \quad (i_t = 1, ..., N_t)$ – and similarly for ρ and z in Eqs. (56)–(57). (This is just the same kind of variation as for the validation test of Sect. 3.4, but here `scale` has a value that is relevant to a galaxy.) Thus, while we browse a very small total interval of time using a very small time step, we do scan a large spatial scale, representative of a disk galaxy. The reason for imposing this difference is that the variation of the fields has a quasi-periodic character in time. This has been checked for the A_z potential by calculating the sum (16) with a very large time step, close to $\delta\rho/c$. Whereas, as we will see below, the fields have a definite spatial variation. On the other hand, the following values were tried for the number N in Eqs. (24)–(30): $N = 6, 12, 24, 48, 96, 192$.

We will compare the field components B_ϕ, E_ρ, E_z, as calculated either "directly", i.e., from Eqs. (50)–(52), or "from the model", i.e., from Eqs. (36)–(38), using in the latter case in Eq. (39) the spectrum values S_{nj} obtained from fitting the sum (16) by Eq. (30), Eq. (35). Thus, in both cases, the field derives from an exact solution Ψ of the scalar wave equation by Eqs. (3) and (4)–(6): Ψ is either the sum (16), or the function (30), which is obtained precisely from fitting the sum (16).

Figures 4 to 9 show, for the $(5, 12, 11)$ spatiotemporal grid, the contour levels of the field components B_ϕ, E_ρ, E_z, as calculated either "directly" or "from the model" – in the latter case, on the same spatiotemporal grid $(5, 12, 11)$ used for the fitting, and with $N = 48$. In order to save place, we selected somewhat arbitrarily, and independently for each component, 3 values of the time among the available 5 values. Also, very similar figures are obtained if one uses another spatiotemporal grid, like $(4, 8, 7)$ or $(7, 14, 13)$.

If the increase of the error with scale, found for the smaller scales investigated in the validation test of Subsect. 3.4 (up to $10^3\lambda$), would continue up to the scale relevant to a typical disc galaxy ($\simeq 3 \times 10^{25}\lambda$), then the relative quadratic errors between the field components calculated either directly or from the model (e.g. $\parallel \delta B_\phi \parallel / \parallel B_\phi \parallel$) would reach huge values for the galactic scale that we are investigating in this section. For the validation test, the increase of the error with scale was due to the fact that the discretization number N was not increased in proportion of the scale length. The exact spectrum (14) was available, and the discretized spectrum values were taken from it, Eq. (43). In contrast, in this section, the discretized spectrum values S_{nj} are now obtained from fitting the sum (16) by Eq. (30). For the present calculation, the relative quadratic errors are rather close to unity. The qualitative features of the fields are the same for the fields calculated directly or with the model, i.e., from the spectra obtained by fitting the A_z potential:

i) The fields are more intense close to the z axis. This feature is true for both the direct calculation and the model, but it appears more clearly with the model. Moreover, using that model, based on Eqs. (36)–(38), one can calculate the three components B_ϕ, E_ρ and E_z also for $\rho = 0$ – which is not the case for the B_ϕ and E_ρ components when one uses the direct calculation based on Eqs. (50)–(52), see after those equations. The model gives $B_\phi = E_\rho = 0$ for $\rho = 0$, because $J_1(0) = 0$. In contrast, for E_z, that model predicts very high values for $\rho = 0$, of the order $E_z = O(10)$ with the spectrum values obtained by fitting the sum (16) by Eq. (30) on the spacetime domain (55)–(57), using e.g. the parameters described in the paragraph following Eqs. (55)–(57) (but using these spectrum values to calculate the fields on a somewhat different grid, starting with $\rho_0 = 0$).

ii) The maximum intensities (positive and negative), calculated either directly or from the model, have quite similar values – but the positions of the maxima are generally different between the direct calculation and the model, except for the fact mentioned, that they are close to the z axis.

An important point has to be noted in this connection. As we saw, the fields have a definite spatial variation at the galactic scale, in contrast to their quasi-periodic time variation with a very small time period $T_0 = \lambda_0/c$. However, to that large-scale spatial variation, is superimposed an oscillatory variation at the very small scale of the main wavelength $\lambda_0 = 0.5\,\mu\text{m}$. This results again from the analytical expressions of the fields, e.g. it is easy to see in Eqs. (36)–(38) for the model. [4] The oscillatory spatial variation at the

[4] However, the same remark applies to the direct calculation, e.g. Eq. (50) for B_ϕ,

wavelength scale implies a high sensitivity of the details of the calculations on a big spatiotemporal grid like (55)–(57) to small variations of the parameters. This is seen, for example, when the spectrum functions S_j obtained from a fitting are used to calculate the fields on a different spatiotemporal grid than the one used for the fitting; or, when two different orders N are used for the same grid. However, the main features of the calculations, as described at points i) and ii) above, are robust, and the relative quadratic differences between different calculations on the same grid usually remain of the order of unity. An exception is if a too low order N is used (e.g. $N = 6$ used to fit and calculate with the model on the $(5, 12, 11)$ grid), in which case larger differences can exist.

Remind that the schematization which leads to the direct calculation (50)–(52) is a rather simple one: an axisymmetric disk-like distribution of point sources, each of which emitting an EM field deriving via Eq. (3) from a spherically symmetric solution Ψ of the scalar wave equation. As we saw at the end of Subsect. 3.3, also the field got from the model is an exact axisymmetric solution of the free Maxwell equations. The set of point-like sources, that may represent a disk galaxy, and that leads directly to the calculation (50)–(52), is also used to adjust the model. The latter, however, is based on the nonsingular ("continuous") equations (30) and (36)–(38) – in contrast with Eqs. (16) and (50)–(52), that are singular at each source (i.e., for $\mathbf{x} = \mathbf{x}_i$). Therefore, the field obtained from the model is at least as representative of the EM field in a disc galaxy as the field calculated directly can be.

5 Conclusion

In this work, an analytical model has been built for the Maxwell field in an axisymmetric galaxy, in particular for that field which results from stellar radiation. This model is based on a representation of any totally propagating axisymmetric free Maxwell field as the sum of two fields given explicitly: in the case of a time-harmonic field, the first field is given by Eqs. (10–(12), and the second one is deduced by the duality (8) from a field of the same

with $B_{\phi\, i}$ given by Eq. (49), where $B_{\phi\, i\, \omega_j}$ is given by Eq. (40) with $\rho'_i, Z_i, r_i, \omega_j, K_j$ in the place of ρ, z, r, ω, K.

form. In a previous work, the general applicability of this representation has been proved.

The model is adjusted by fitting to it the sum of spherical radiations emitted by a set of point-like "stars". The distribution of these point-like objects is axisymmetric. It builds a flat disk, symmetrical with respect to a plane perpendicular to the symmetry axis, and the dimensions have been chosen to represent a disk galaxy similar to the Milky Way. The model provides an exact solution of the free Maxwell equations, also after the discretization that is used to calculate the relevant integrals.

The huge ratio distance/wavelength needs to implement a numerical precision better than the quadruple precision. The model and the corresponding software have passed a validation test based on an exact solution with spherical symmetry. The results for a disk galaxy indicate that the field is highest near to the z axis, and the E_z component dominates over E_ρ. In a further stage it will be possible to adjust the model so as to accurately describe the measured EM spectrum and its spatial variation.

Acknowledgements. I am grateful to Christian Boily and to Garrelt Mellema for useful remarks at the Computational Astrophysics Conference in Saint Petersburg, September 2019.

References

[1] Beck, R.; Wielebinski, R. Magnetic Fields in the Milky Way and in Galaxies. In *Planets, Stars and Stellar Systems, Vol. 5: Galactic Structure and Stellar Populations*; Oswalt, T.D., Gilmore, G., Eds.; Springer: Berlin, 2013; Chapter 13, pp. 641–723; DOI: 10.1007/978-94-007-5612-0_13.

[2] Chamandy, L.; Subramanian, K.; Shukurov, A. Galactic Spiral Patterns and Dynamo Action I: A New Twist on Magnetic Arms. *Mon. Not. R. Astron. Soc.* **2013**, *428*, 3569–3589; DOI: 10.1093/mnras/sts297.

[3] Porter, T. A.; Strong, A. W. A New Estimate of the Galactic Interstellar Radiation Field between 0.1μm and 1000μm. In *29th International Cosmic Ray Conference, Pune*; Tata Institute of Fundamental Research: Mumbai, India, 2005; Vol. 4, pp. 77-80.

[4] Maciel, W. J.; The Interstellar Radiation Field. In *Astrophysics of the Interstellar Medium*; Maciel, W. J., Ed.; Springer: New York, 2013; Chapter 2, pp. 17-31; DOI: `10.1007/978-1-4614-3767-3_2`.

[5] Kent, S. M.; Dame, T. M.; Fazio, G. Galactic Structure from the Spacelab Infrared telescope. II. Luminosity Models of the Milky Way. *Astroph. J.* **1991**, *378*, 131–138; DOI:10.1086/170413.

[6] Robin, A. C.; Crézé, M.; Mohan, V. The Radial Structure of the Galactic Disc. *Astron. Astrophys.* **1992**, *265*, 32–39.

[7] Porcel, C.; Garzón, F.; Jiménez-Vicente, J. The Radial Scale Length of the Milky Way. *Astron. Astrophys.* **1998**, *330*, 136–138.

[8] Arminjon, M. On the Equations of Electrodynamics in a Flat or a Curved Spacetime and a Possible Interaction Energy. *Open Physics* **2018**, *16*, 488–498; DOI: 10.1515/phys-2018-0065.

[9] Arminjon, M. Space Isotropy and Weak Equivalence Principle in a Scalar Theory of Gravity. *Braz. J. Phys.* **2006**, *36*, 177–189; DOI: 10.1590/S0103-97332006000200010.

[10] Zamboni-Rached, M.; Recami, E.; Hernández-Figueroa, H. E. Structure of Nondiffracting Waves and Some Interesting Applications. In *Localized Waves*; Hernández-Figueroa, H. E., Zamboni-Rached, M., Recami, E., Eds.; John Wiley & Sons: Hoboken, 2008; DOI: 10.1002/9780470168981.ch2.

[11] Garay-Avendaño, R. L.; Zamboni-Rached, M. Exact Analytic Solutions of Maxwell's Equations Describing Propagating Nonparaxial Electromagnetic Beams. *Appl. Opt.* **2014**, *53*, 4524–4531; DOI: 10.1364/AO.53.004524.

[12] Arminjon, M. An Explicit Representation for the Axisymmetric Solutions of the Free Maxwell Equations. *Open Physics* **2020**, *18*, 255–263; DOI: 10.1515/phys-2020-0117.

[13] Gradshteyn, I. S.; Ryzhik, I. M. *Table of Integrals, Series, and Products*, 7th English Edition. Burlington (Mass., USA): Academic Press, 2007; §6.677, p. 722.

[14] Atkinson, K. E. *An Introduction to Numerical Analysis*, 2nd Edition. New York: John Wiley & Sons, 1989; pp. 257–258.

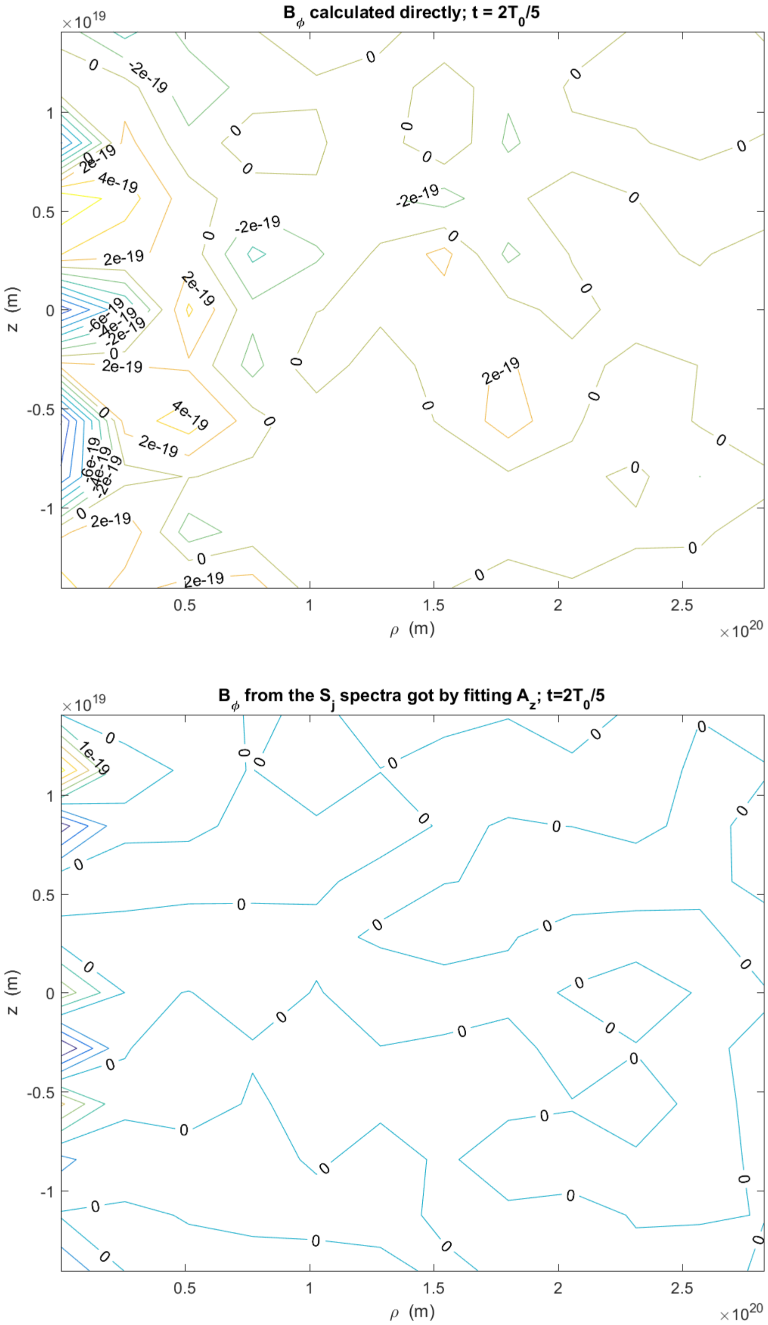

Figure 4: B_ϕ calculated directly or from the model; $t = 2T_0/5$

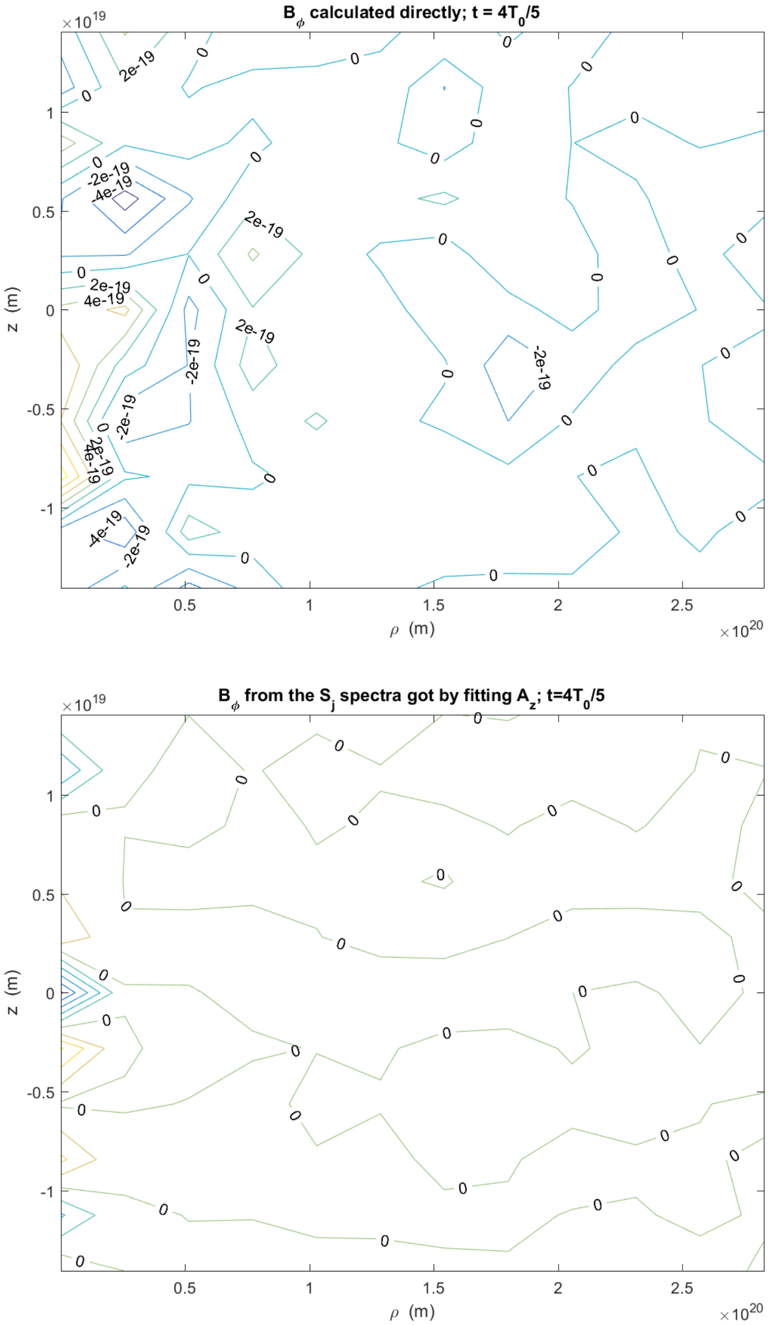

Figure 5: B_ϕ calculated directly or from the model; $t = 4T_0/5$

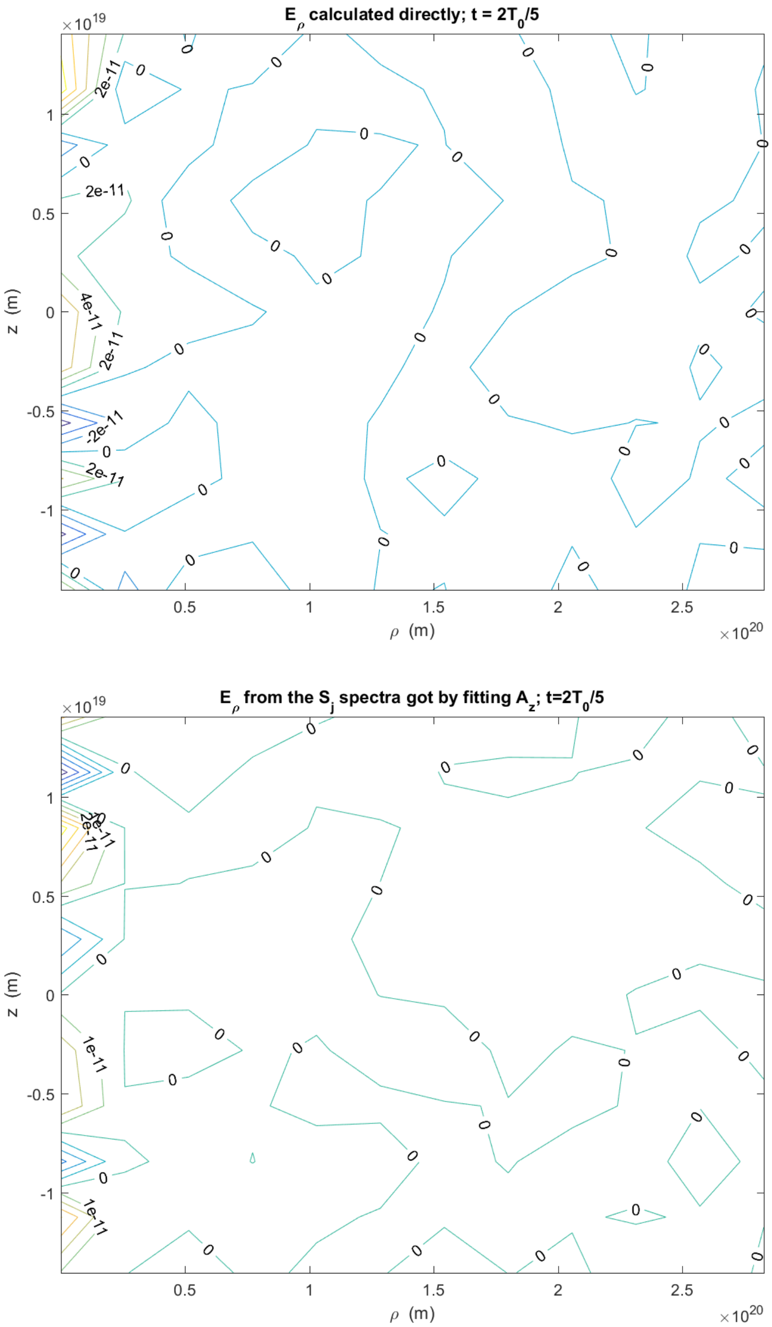

Figure 6: E_ρ calculated directly or from the model; $t = 2T_0/5$

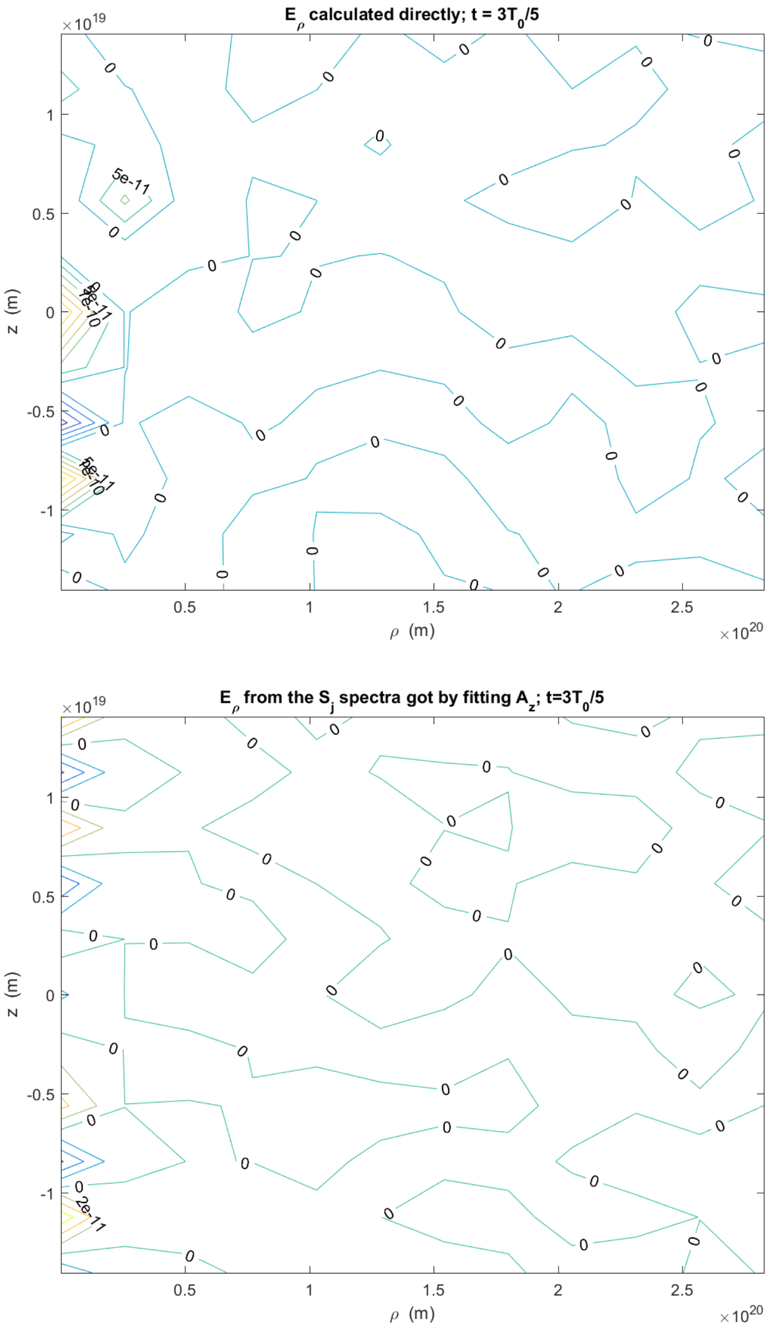

Figure 7: E_ρ calculated directly or from the model; $t = 3T_0/5$

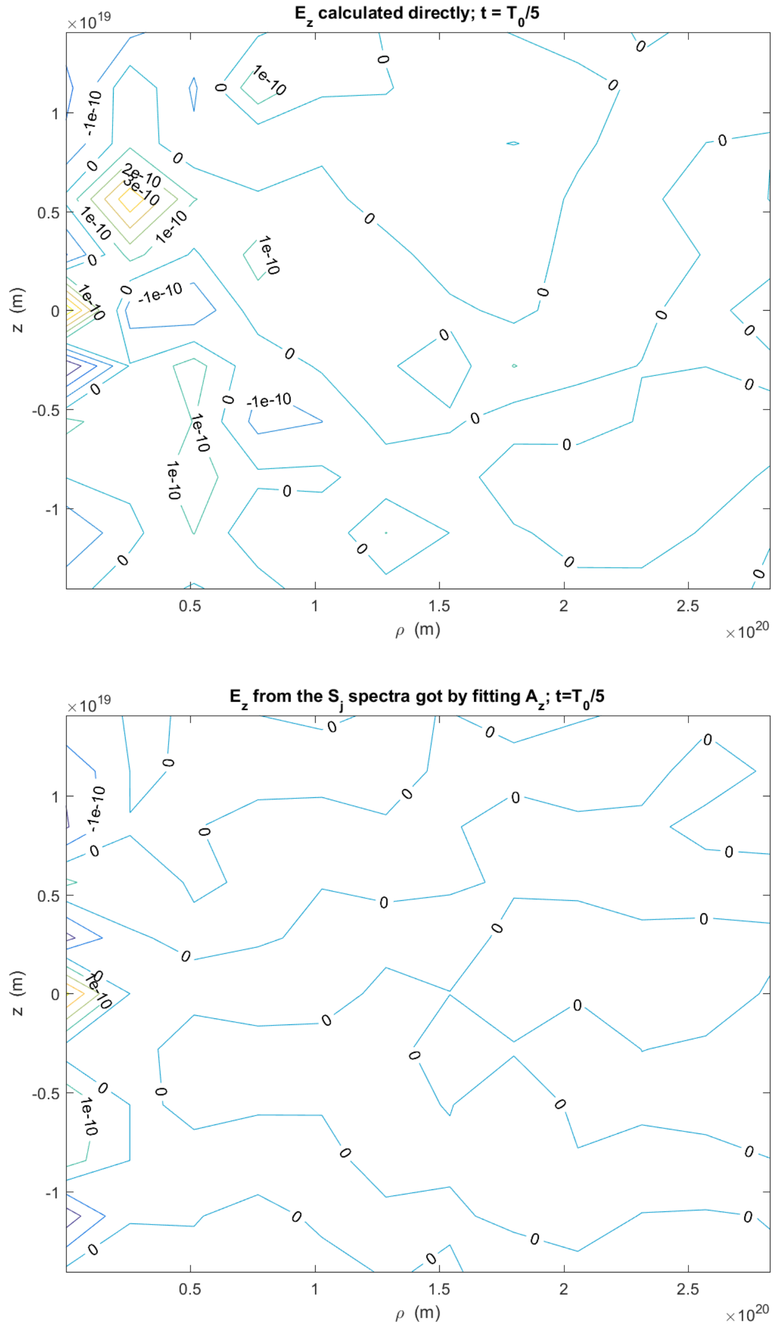

Figure 8: E_z calculated directly or from the model; $t = T_0/5$

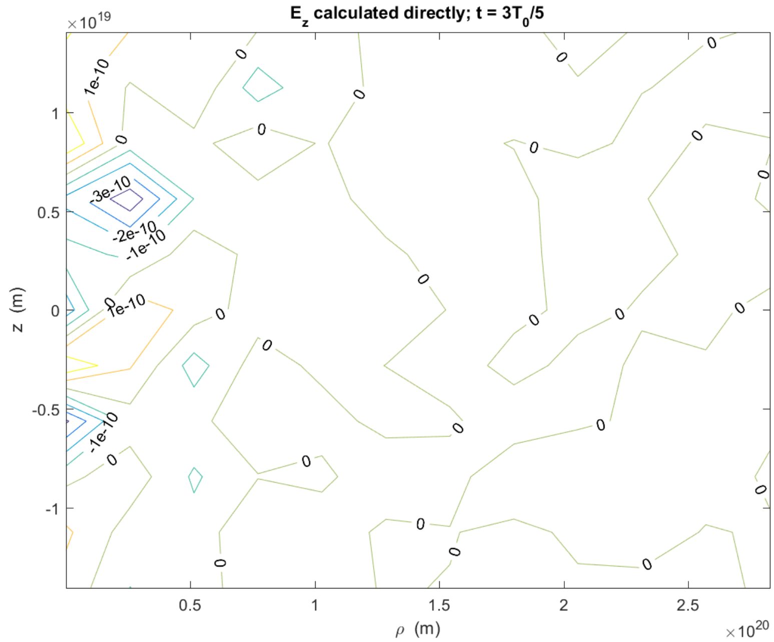

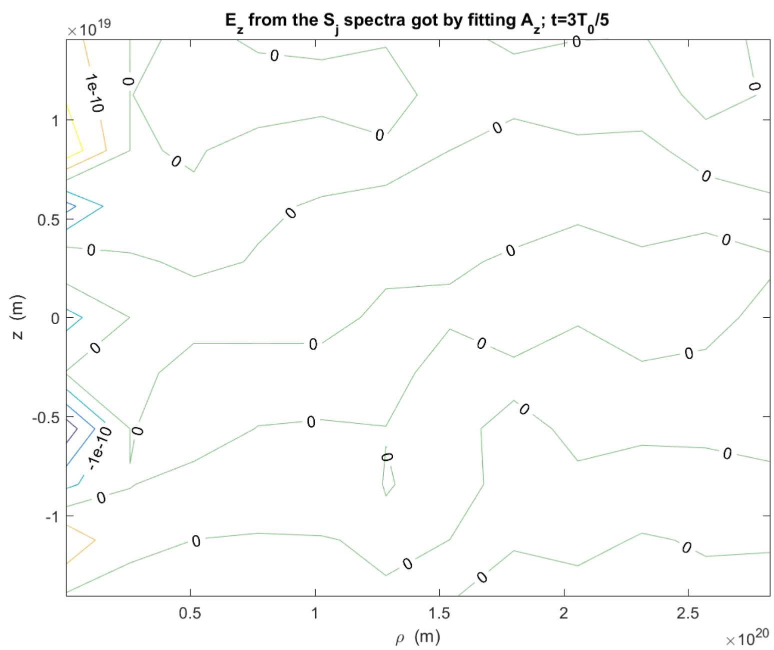

Figure 9: E_z calculated directly or from the model; $t = 3T_0/5$